SUPPLEMENTARY FIGURES AND TABLES

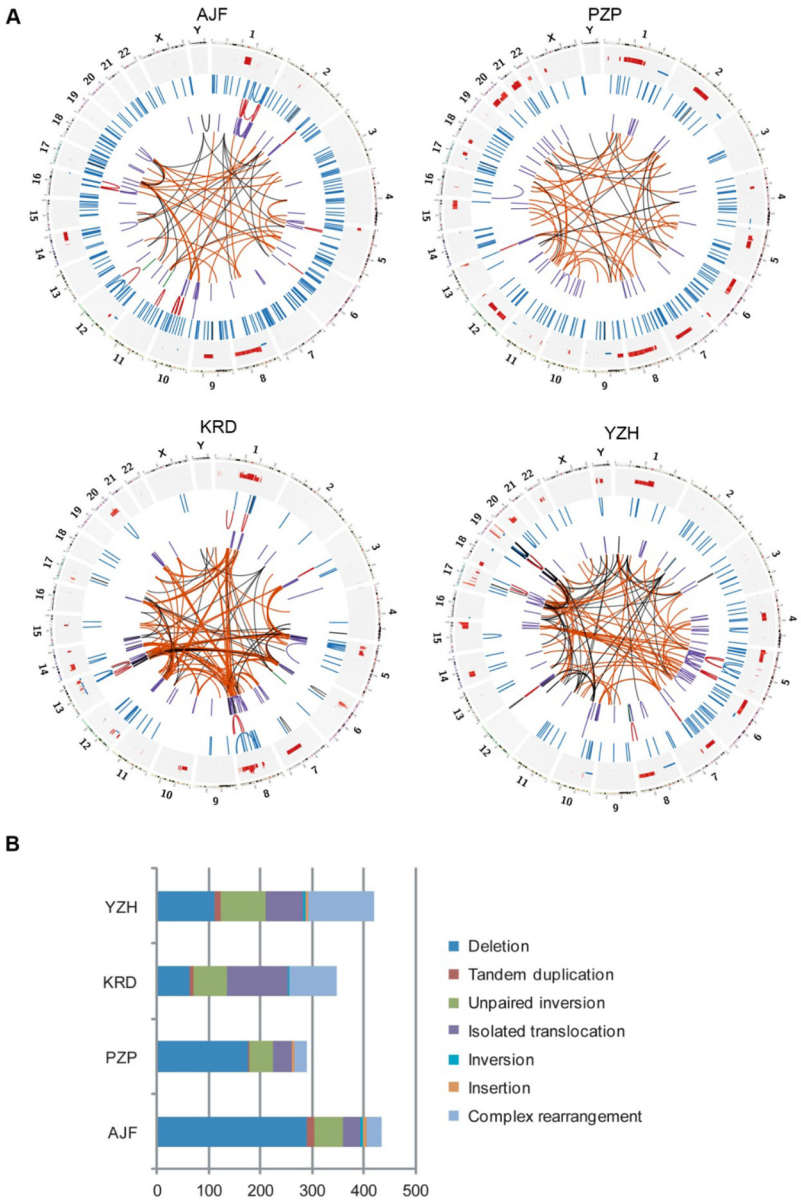

Supplementary Figure S1: Genome rearrangements of four primary OS analyzed by DNA-PET sequencing. **(A)** Genomic SVs enriched for somatic events identified by genome-wide mate-pair sequencing of long DNA fragments of four OS tumors are displayed by Circos [1]. The human genome is arranged in a circle with the chromosome number and the cytogenetic bands displayed in the outer ring, the somatic copy number alterations in the next inner concentric ring (red, amplifications; blue, deletions), followed by deletions, tandem duplications, inversions/unpaired inversions, and in the center of the circle inter-chromosomal rearrangements. Isolated and complex inter-chromosomal rearrangements are represented by orange and black lines, respectively. **(B)** Distribution of SV categories which are enriched for somatic events in the four OS tumors shown in A, X-axis indicates absolute numbers of color coded SV types as described in the legend.

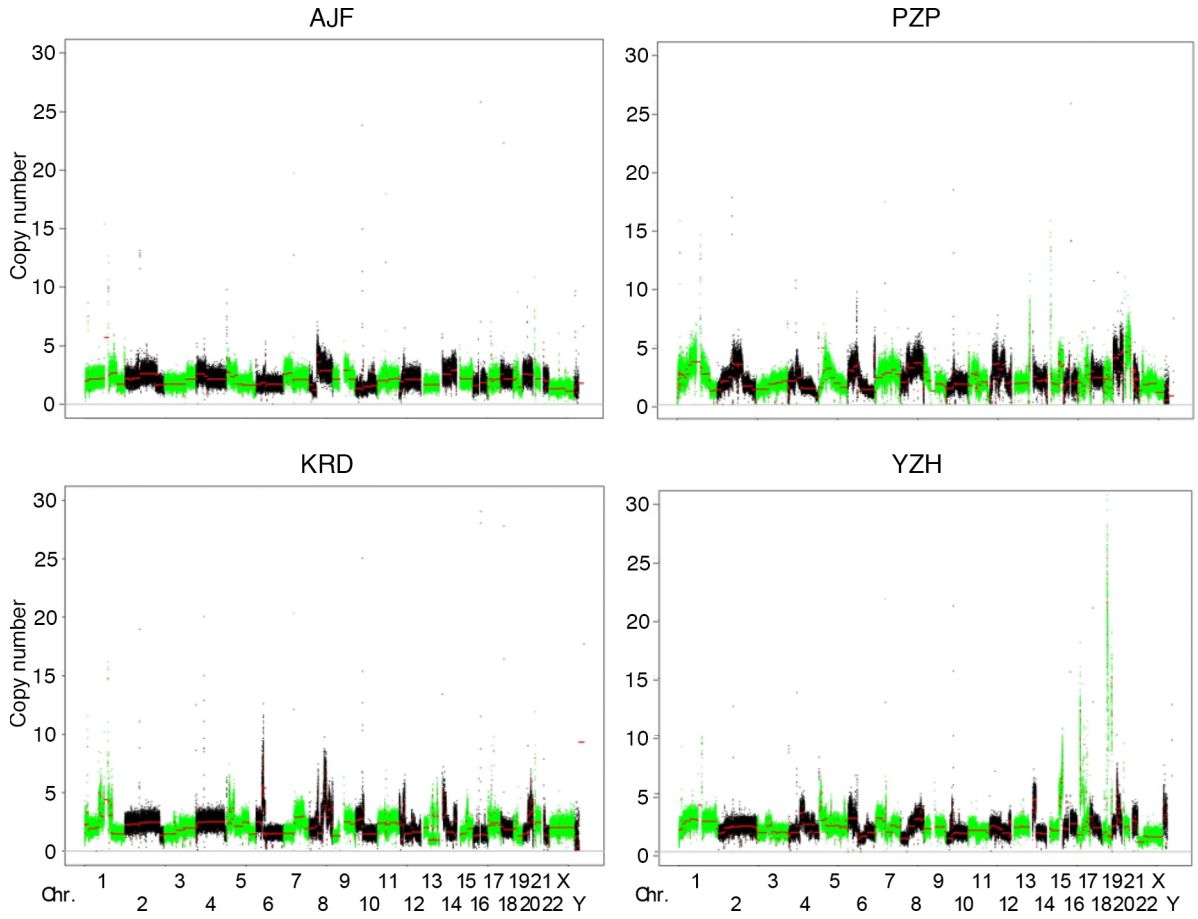

Supplementary Figure S2: Copy number profile of four primary OS derived from DNA-PET sequencing. Chromosomes are aligned on the x-axis and copy number values are on the y-axis. All four OS display a large number of copy number alterations.

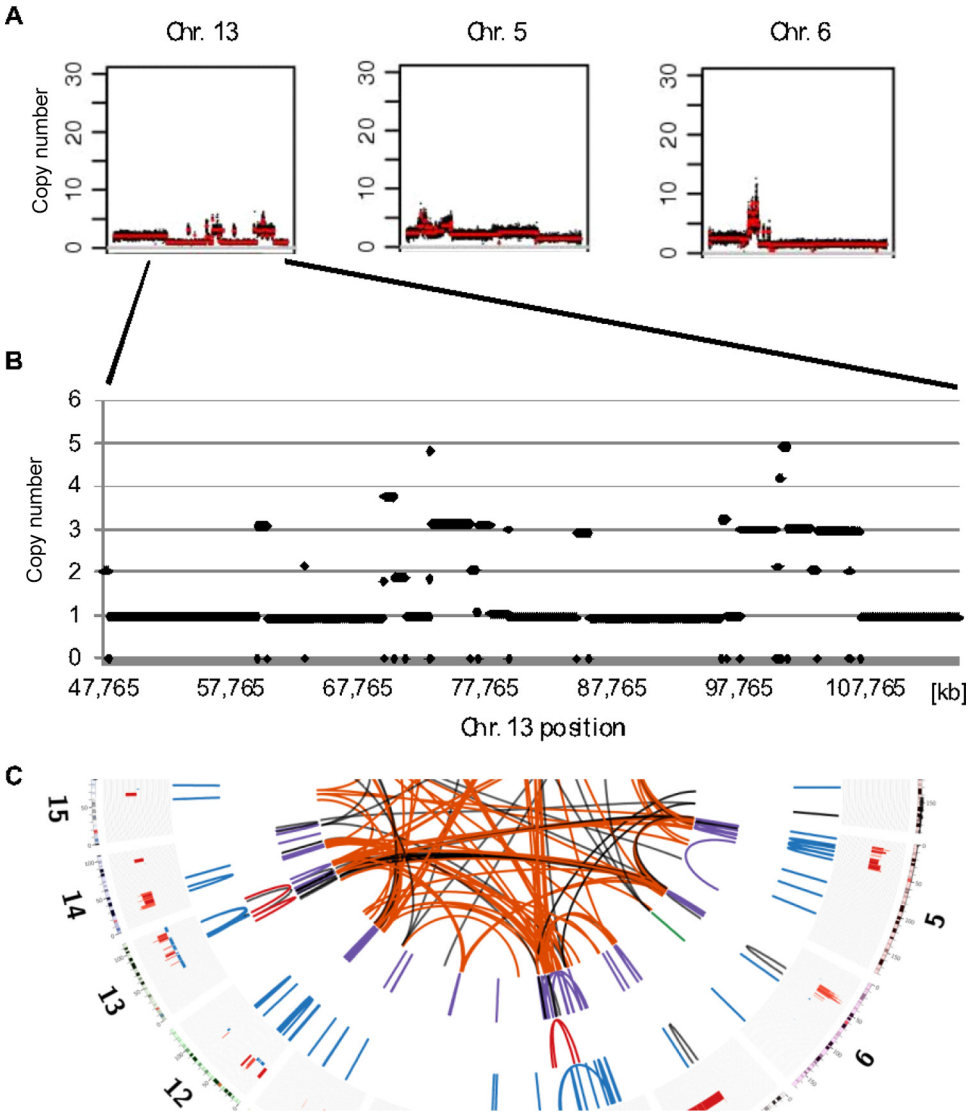

Supplementary Figure S3: Evidence for chromothripsis in OS tumor KRD. **(A)** Copy number profiles of chromosomes 13, 5 and 6 derived from concordant mapping paired-end tag sequencing data relative to simulation control. Chromosomes are aligned on the x-axes and copy number values are on the y-axes. Black dots indicate copy number based on 10 kb windows. Red lines are smoothened copy number across neighboring windows. **(B)** Enlarged copy number profile of chromosome 13 positions 47.7 Mb to 115.1 Mb. Data points are based on 10 kb windows. **(C)** Capture of genomic Circos plot [1] including chromosomes 13, 5 and 6. Information displayed in the concentric rings is as follows from outside to inside: chromosome number; cytogenetic banding, copy number with gains in red and losses in blue; deletions; tandem duplications; inversions/unpaired inversions; inter-chromosomal rearrangements. Color coding for inter-chromosomal SVs is indicated in orange and inter-chromosomal SVs in complex regions in black.

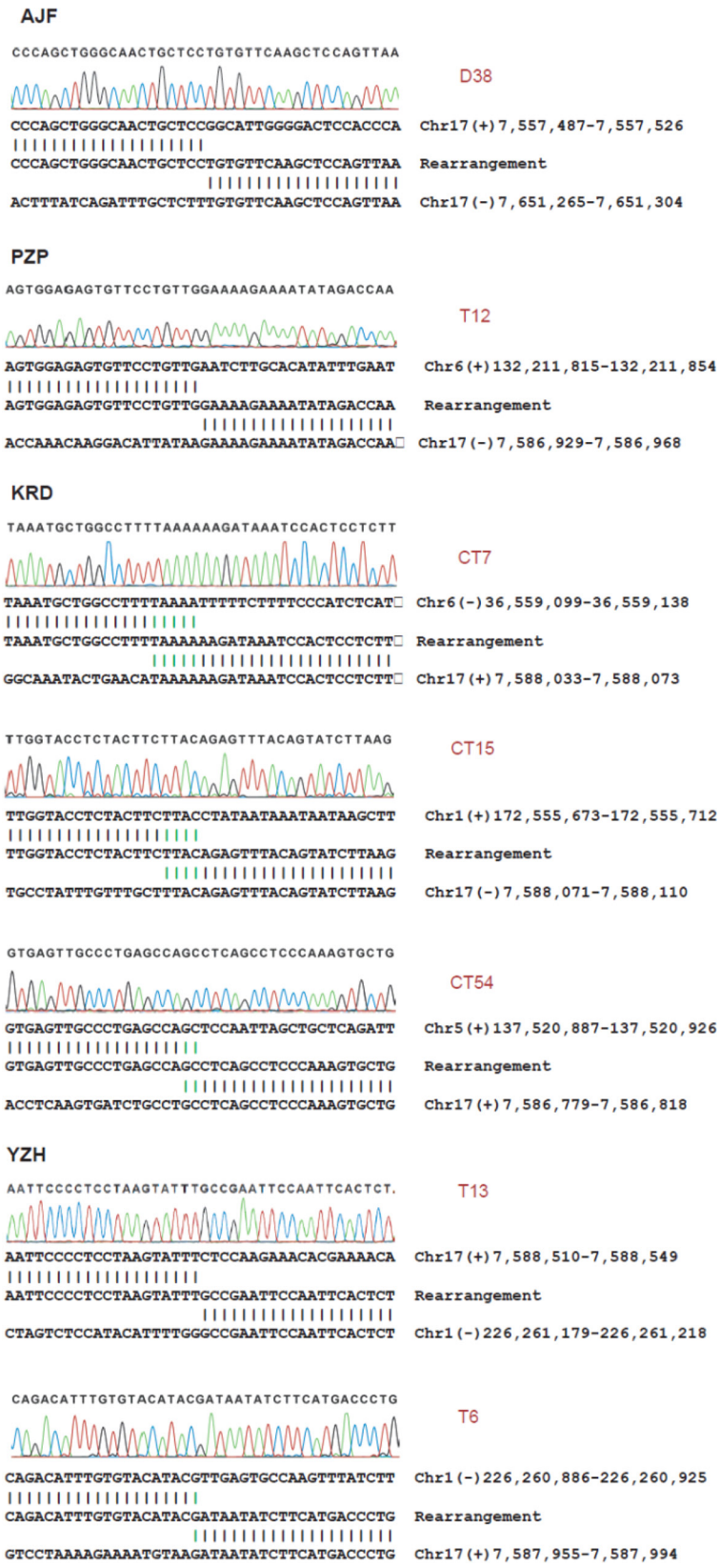

Supplementary Figure S4: Validation of *TP53* rearrangements by PCR and Sanger sequencing. Patient IDs are indicated in bold capital letters. Bases matching between the rearrangement and the reference sequences of the participating regions are indicated by vertical lines. Micro homologies between the two participating break point regions are illustrated by green vertical lines. Break point IDs are shown in red.

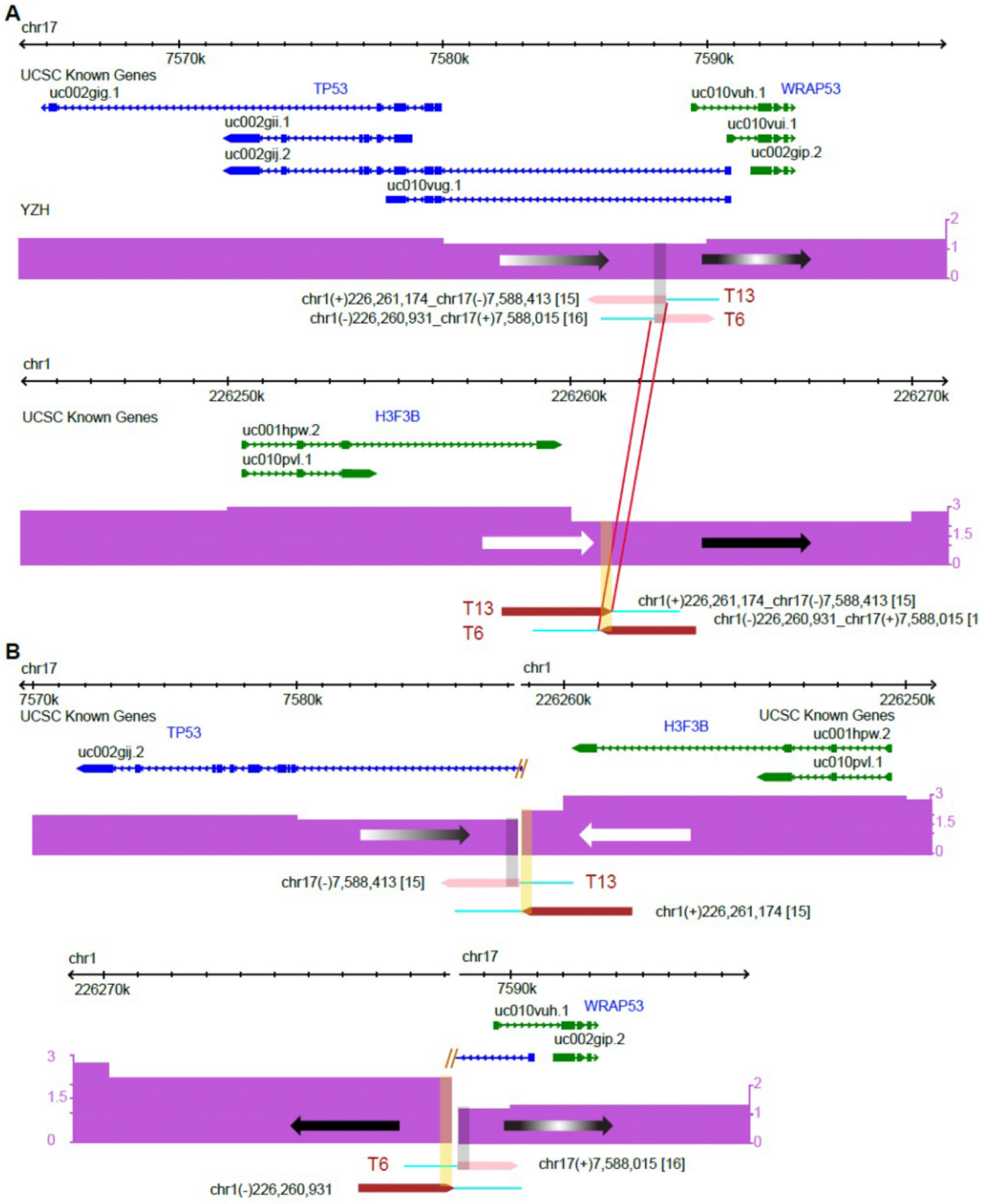

Supplementary Figure S5: Balanced translocation between intron 1 of *TP53* and a locus on chromosome 1 in OS patient YZH. (A) Chromosome 17 and 1 loci of the human reference genome (hg19) which show the PET mapping regions indicating the balanced translocation between the two loci. Genes showing the major splice variants derived from the UCSC known genes database [2] are shown on top and smoothened copy number information derived from DNA-PET sequencing data is shown at the bottom (purple tracks) in the Genome Browser. Genes transcribed from the plus strand are represented in green, genes transcribed from the minus strand are represented in blue. Boxes indicate exons, barbed lines indicate introns. Mapping regions of 5' and 3' PET clusters and read orientations are indicated by dark red and pink arrow heads, respectively, with turquois lines indicating the side of breakpoint. Gray and yellow shading indicate sequences of 555 bp and 293 bp which are shared by both sides of the balanced translocation product for chromosome 17 and 1, respectively. Red lines indicate connectivity between the two chromosomes. Note that DNA-PET coordinates differ from the exact break point coordinates which have been determined by PCR and Sanger sequencing and which are shown in Table S7. **(B)** Translocation outcome as indicated by DNA-PET truncating *TP53* and duplicating gray and yellow shaded sequences.

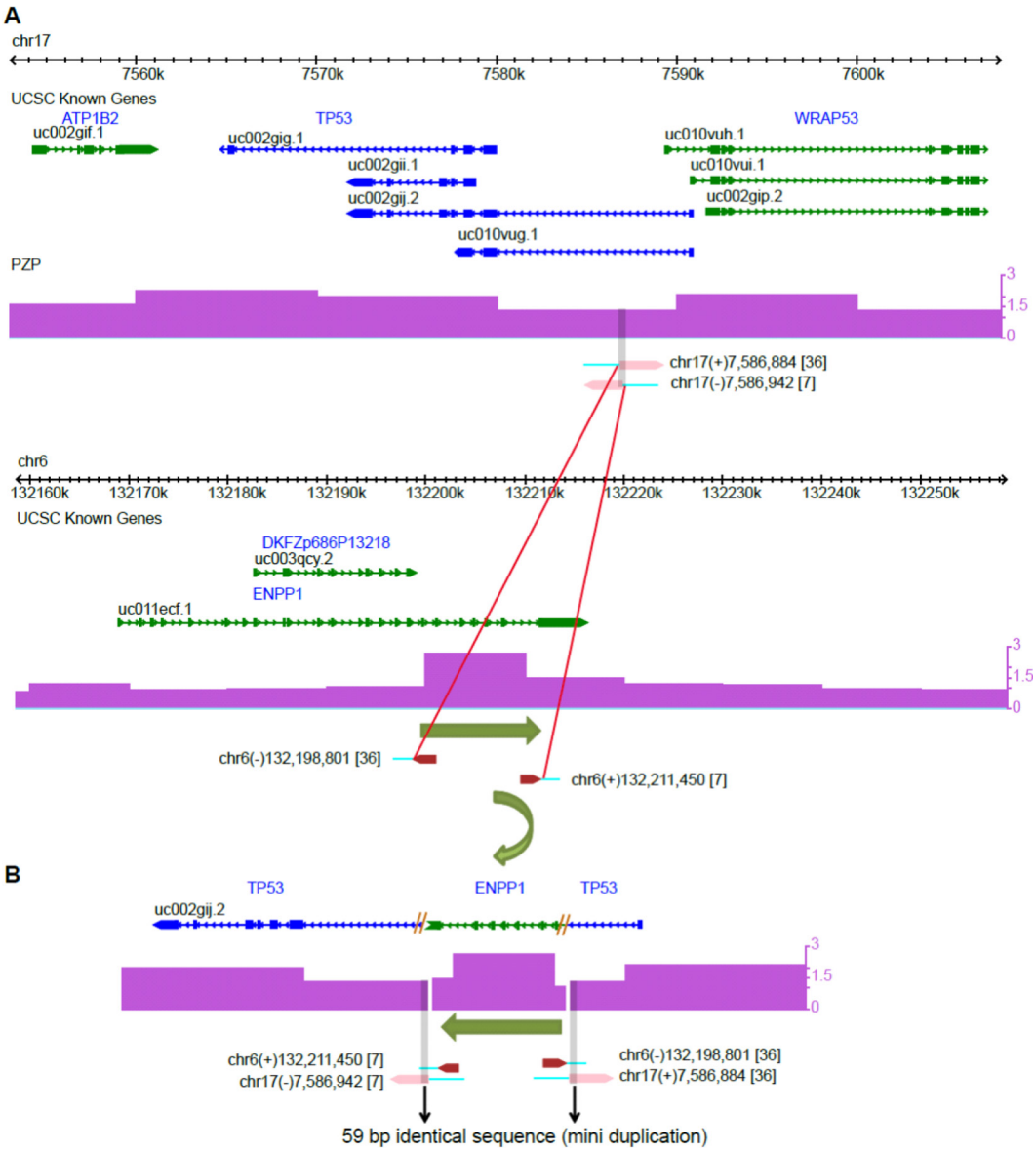

Supplementary Figure S6: Inverted insertion of 12.5 kb of chromosome 6 into intron 1 of *TP53* in OS patient PZP. Identification of an inverted insertion originating from chromosome 6 containing *ENPP1* exon 19 to the 5' part of exon 25 into intron 1 of *TP53* by DNA-PET. For more detailed track information, see legend of Supplementary Figure S5, for exact break point coordinates, see Table S7. **(A)** Chromosome 17 and 6 loci of the human reference genome (hg19) which show the PET mapping regions indicating the inverted insertion. **(B)** Insertion outcome as indicated by DNA-PET creating a potential fusion transcript between exon 1 of *TP53* (right blue box) and exon 19 to the first part of exon 25 of *ENPP1*. Since exon 1 of *TP53* is non-coding, and the inserted part of *ENPP1* exon 25 contains a stop codon, the formation of a fusion protein is unlikely.

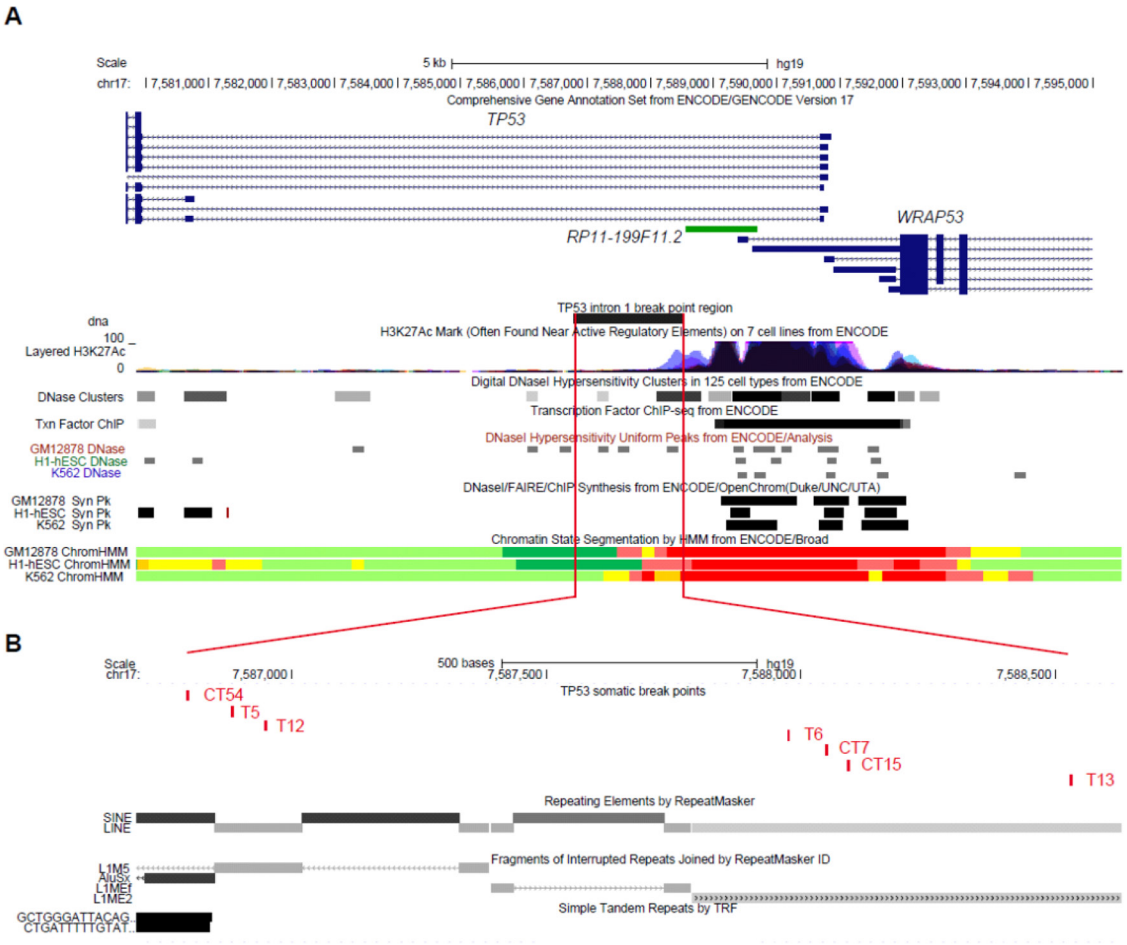

Supplementary Figure S7: *TP53* break point cluster region is located near sites of active chromatin and DNA breaks occur in LINE sequences. UCSC genome browser view (http://genome.ucsc.edu/; [2]) of the *TP53* intron 1 locus. **(A)** ENCODE epigenetic information is derived from the analysis of commonly used cell lines [3]. Tracks from top to bottom are: gene annotation after exclusion of 'problematic' transcripts; user track indicating the break point cluster region; histone 3 lysine 27 acetylation (H3K27ac) chromatin immunoprecipitation-sequencing (ChIP-seq) of seven cell lines as a superimposed layered track suggests active regulatory sites; DNaseI hypersensitive sites derived from ChIP-seq and a uniform peak analysis represent open chromatin; integrated active chromatin information prediction of DNaseI hypersensitivity, formaldehyde-assisted isolation of regulatory elements (FAIRE), and ChIP-seq of three cell lines; chromatin state segmentation analysis: dark red = active promoter, light red = weak promoter, orange = strong enhancer, yellow = weak/poised enhancer, dark green = transcriptional transition/elongation, light green = weak transcription. **(B)** *TP53* intron 1 break points are indicated by red vertical lines and IDs. Below are UCSC track information on repetitive DNA sequences.

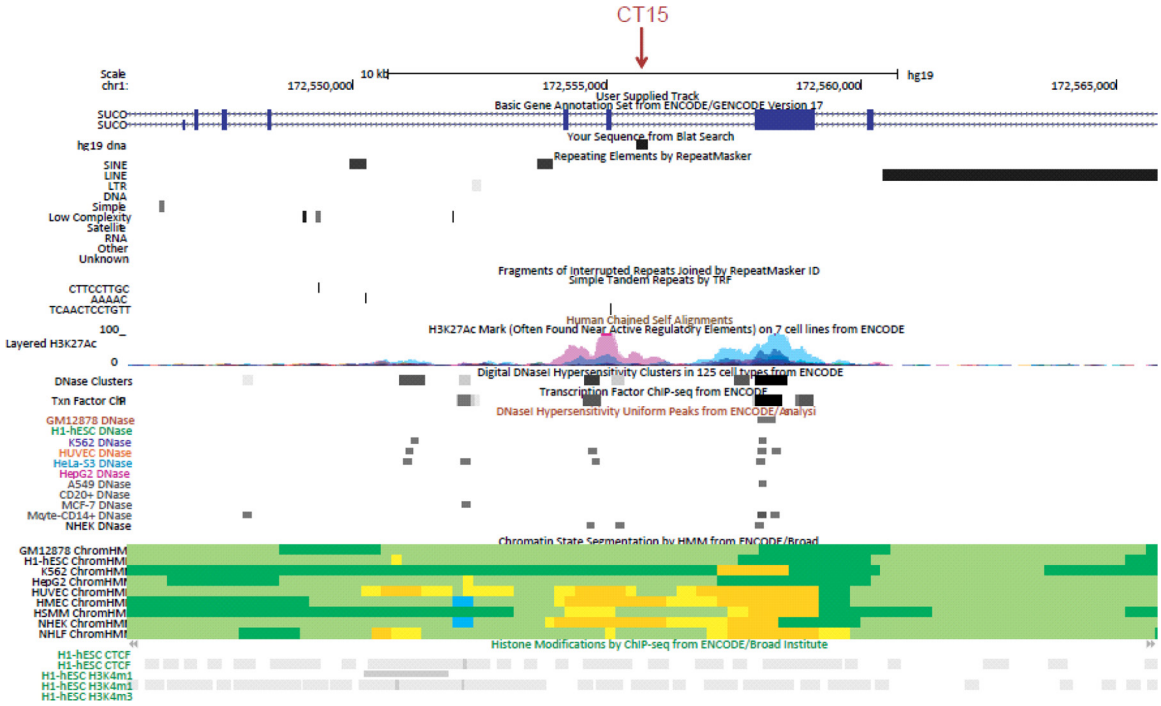

Supplementary Figure S8: Regulatory information of translocation partner site on chromosome 1 of *TP53* translocation in OS patient KRD. UCSC genome browser view of repetitive sequences and ENCODE regulatory information. Break point location is indicated by red arrow. For track description, see legend of Supplementary Figure S7.

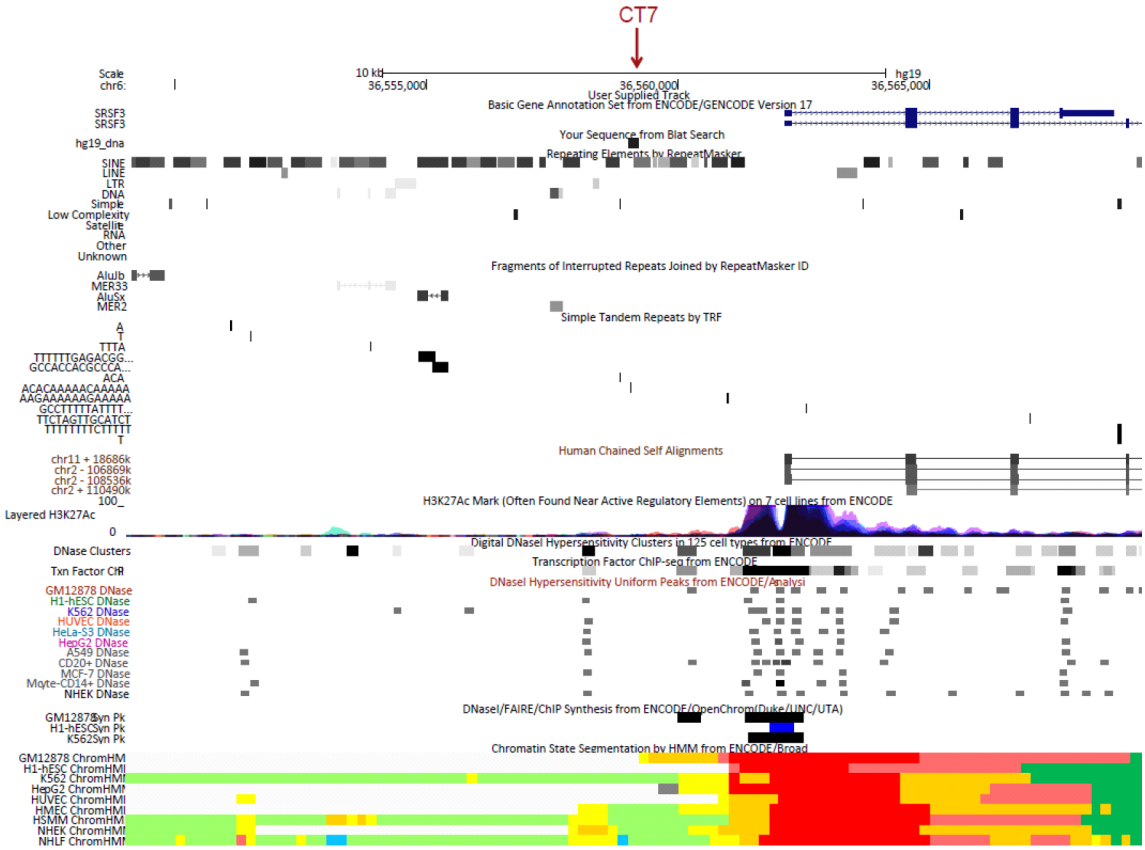

Supplementary Figure S9: Regulatory information of translocation partner site on chromosome 6 of *TP53* translocation in OS patient KRD. UCSC genome browser view of repetitive sequences and ENCODE regulatory information. Break point location is indicated by red arrow. For track description, see legend of Supplementary Figure S7.

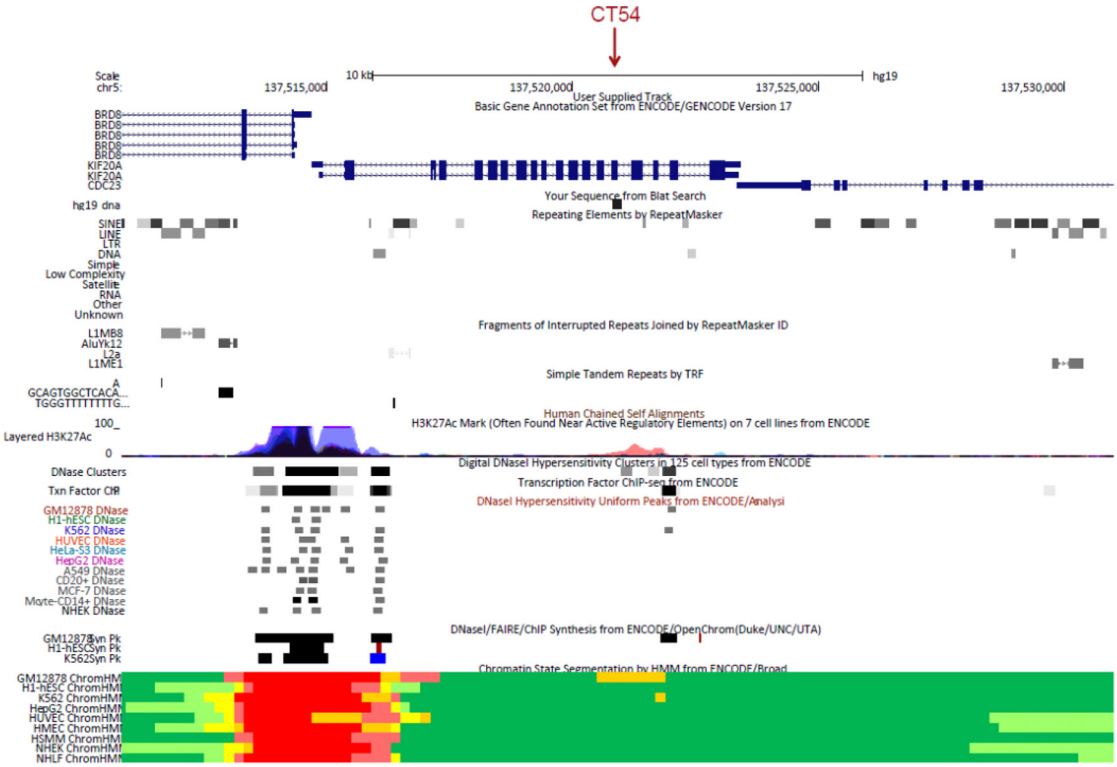

Supplementary Figure S10: Regulatory information of translocation partner site on chromosome 5 of *TP53* translocation in OS patient KRD. UCSC genome browser view of repetitive sequences and ENCODE regulatory information. Break point location is indicated by red arrow. For track description, see legend of Supplementary Figure S7.

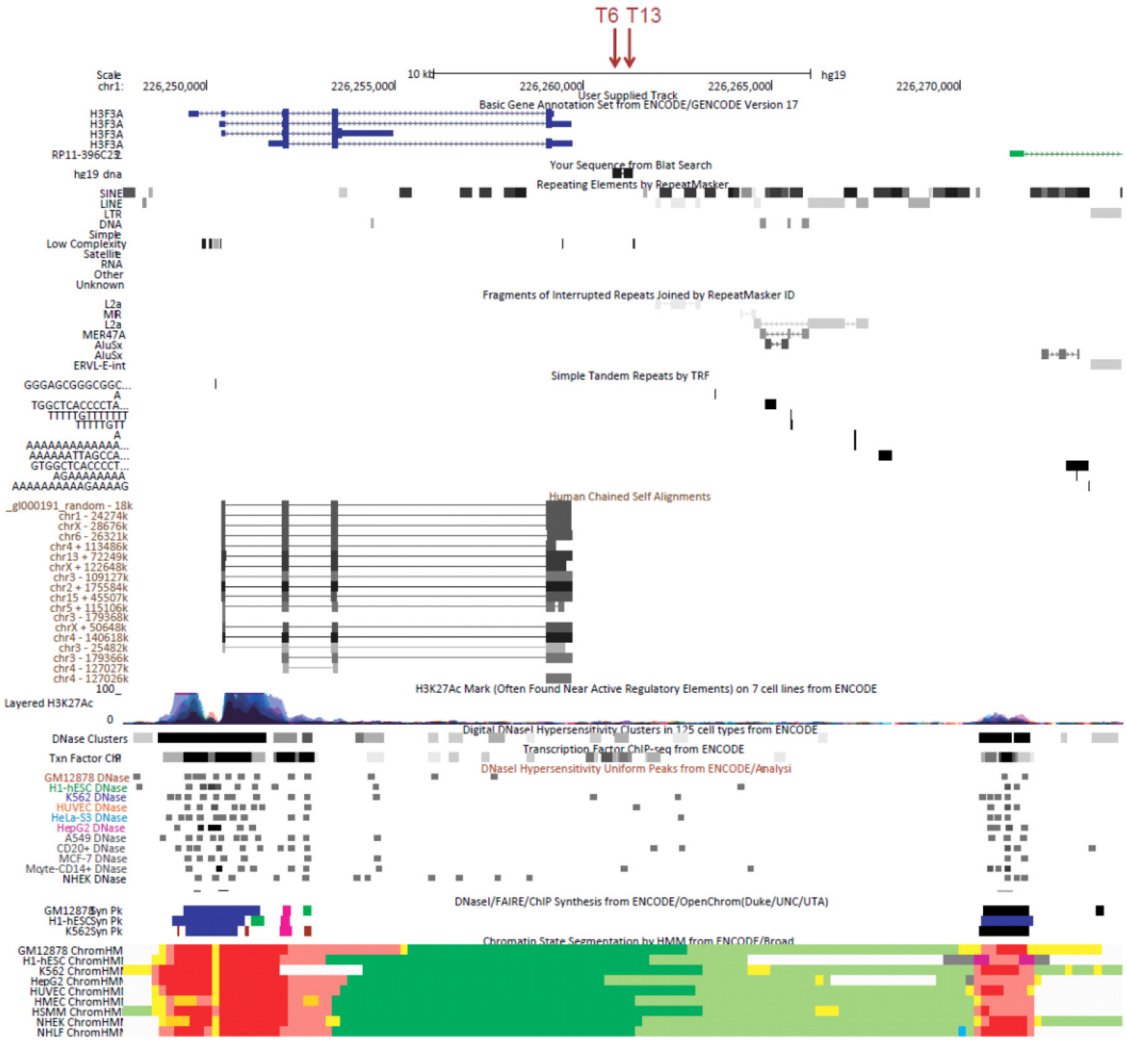

Supplementary Figure S11: Regulatory information of partner site on chromosome 1 of *TP53* balanced translocation in OS patient YZH. UCSC genome browser view of repetitive sequences and ENCODE regulatory information. Break point locations are indicated by red arrows. For track description, see legend of Supplementary Figure S7.

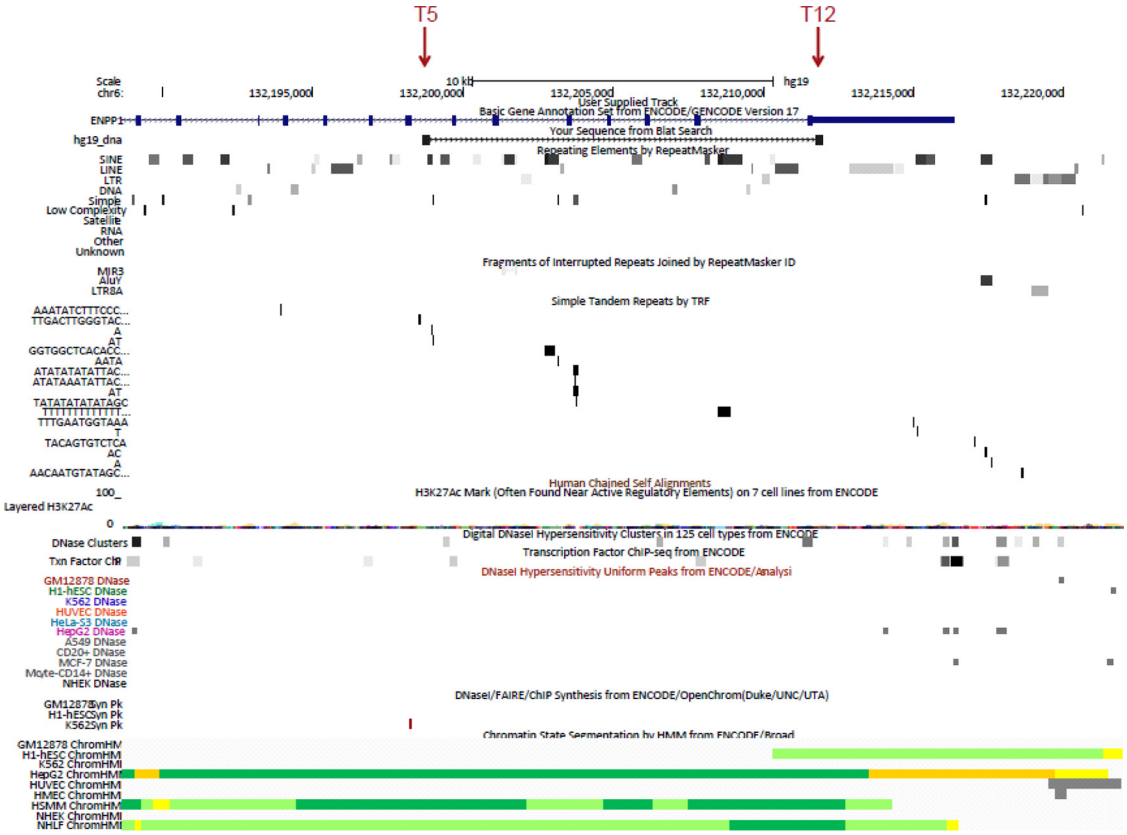

Supplementary Figure S12: Regulatory information of genomic region on chromosome 6 which got inserted into *TP53* in OS patient PZP. UCSC genome browser view of repetitive sequences and ENCODE regulatory information. Break points of the 12.5 kb segment which got inserted into intron 1 of *TP53* are indicated by red arrows. For track description, see legend of Supplementary Figure S7.

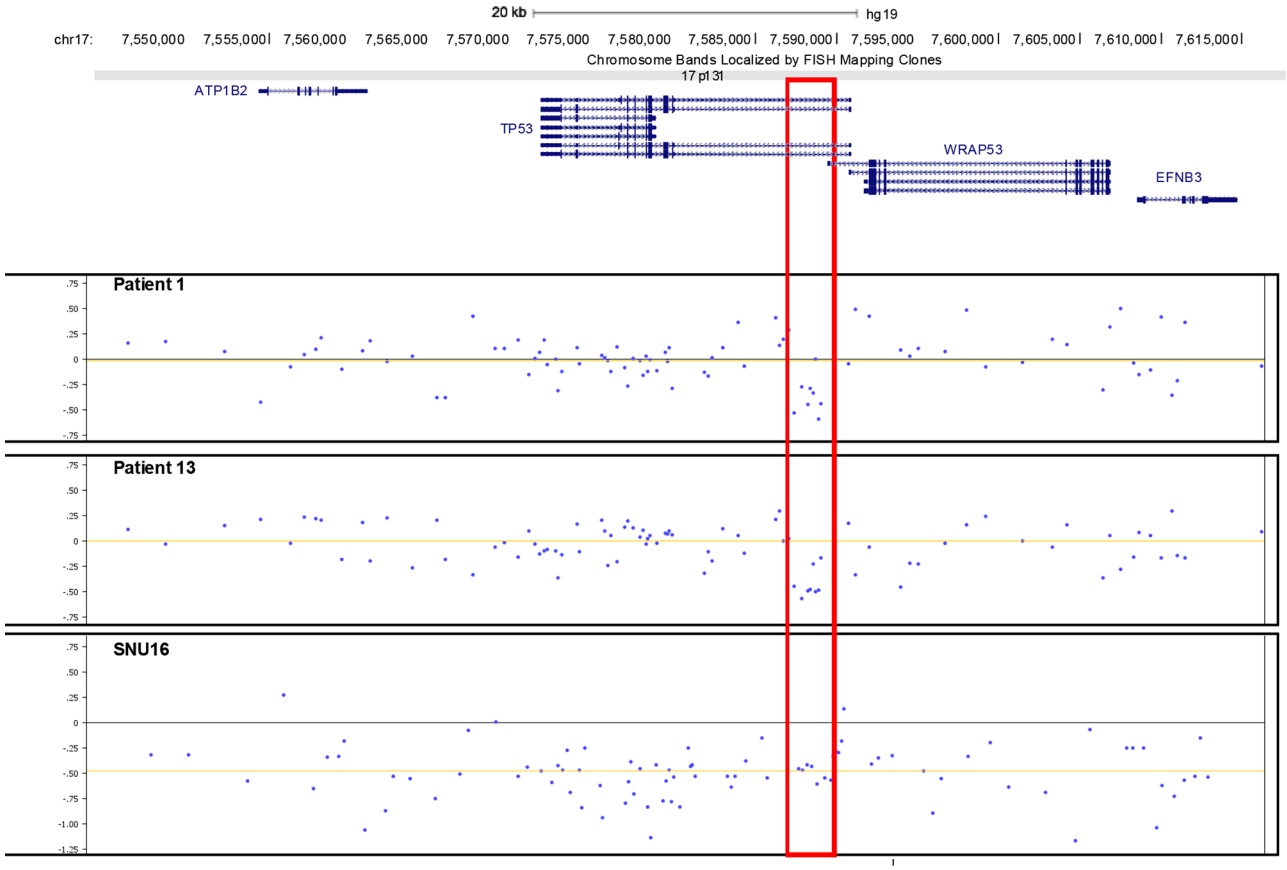

Supplementary Figure S13: Copy number analysis of the *TP53* locus of LFS family members 1 and 13 by CytoScan array. CytoScan array derived copy number analysis of LFS patients 1 and 13 and as copy number loss control gastric cancer cell line SNU16. Gene content of chr17:7,544,275..7,619,275 (NCBI genome build 37) is shown on top, log2 ratios of genomic marker intensities (y-axis) are displayed across the locus (x-axis). SNU16 has a heterozygous deletion of the entire locus (log2 ratio ca. 0.5) and intensities of seven markers of patients 1 and 13 show lower intensities (log2 ratio ca. 0.5, red box) which was not called by Chromosome Analysis Suite version CytoB-N1.2.2.271 (r4615; Affymetrix).

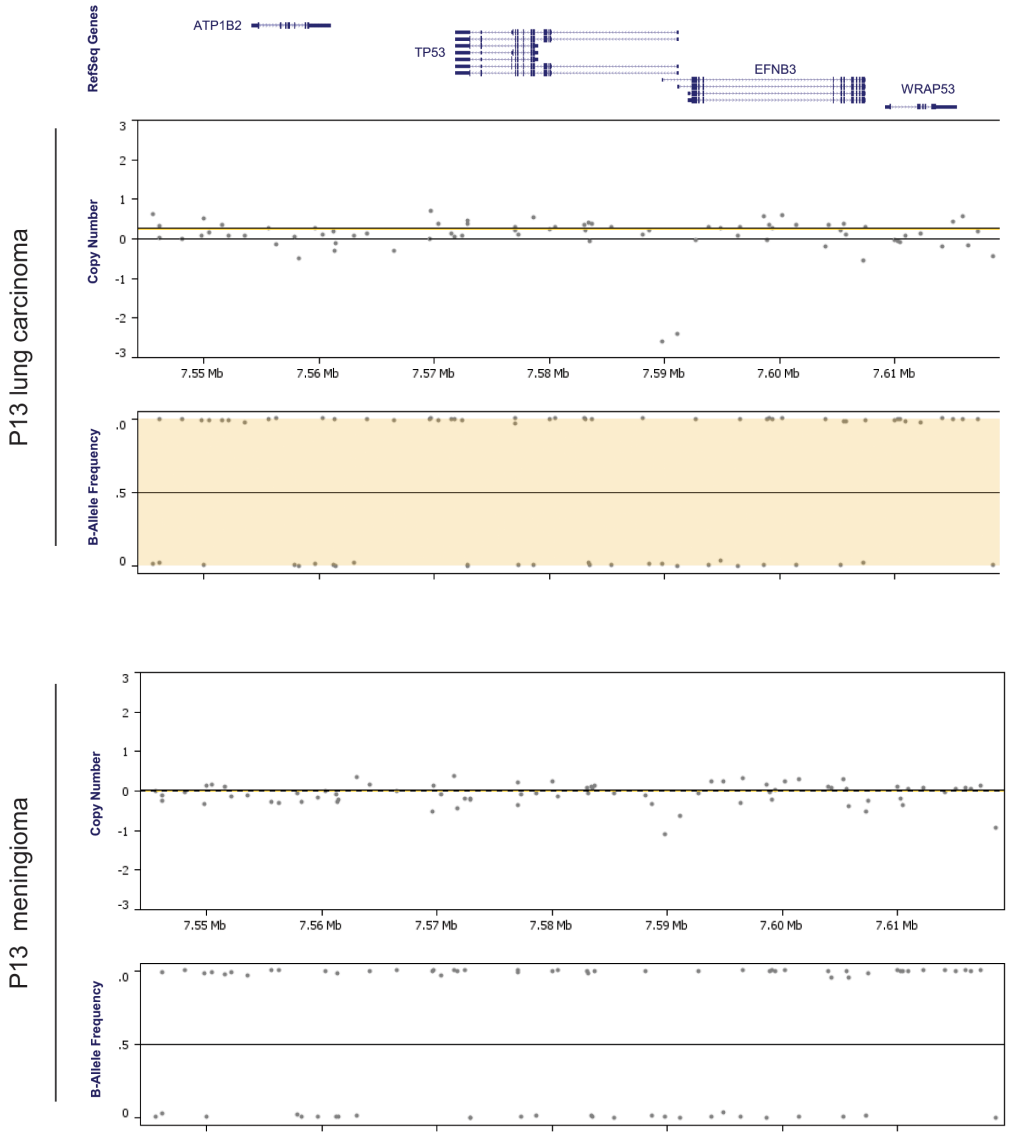

Supplementary Figure S14: Copy number analysis of the *TP53* locus of two tumors of LFS family member P13 by OncoScan array. OncoScan array derived copy number analysis of lung carcinoma and meningioma of LFS patient P13. Gene content of chr17:7,544,000..7,618,000 (NCBI genome build 37) is shown on top, log2 ratios of genomic marker intensities (y-axis) are displayed across the locus (x-axis). Copy number ratio relative to control indicates the presence of two chromosome copies and B allele frequency shows only homozygous variant calls with frequencies close to 1 or 0, respectively, indicating LOH.

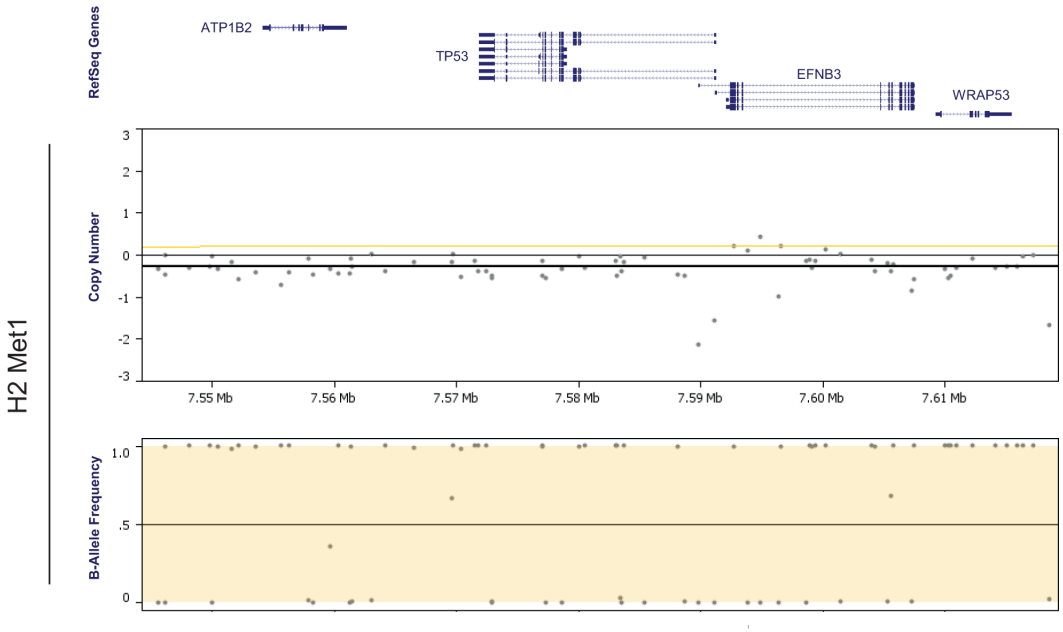

Supplementary Figure S15: Copy number analysis of the *TP53* locus of metastasis of LFS family member H2 by OncoScan array. OncoScan array display is as described for Supplementary Figure S14.

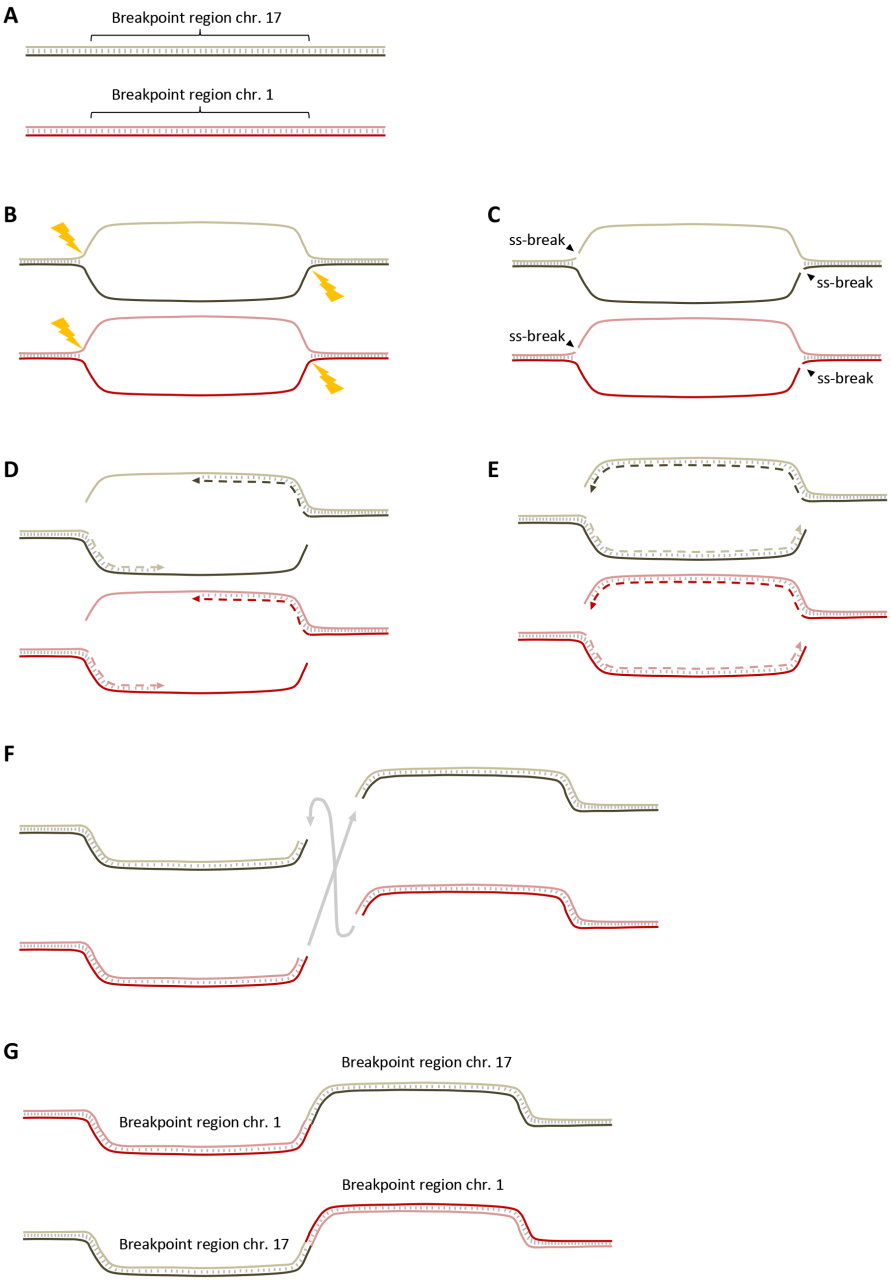

Supplementary Figure S16: Hypothetical *TP53* intron 1 rearrangement mechanism in OS. Schematic representation of a hypothetical rearrangement mechanism that can explain the duplication of 46 bp to 555 bp flanking the *TP53* intron 1 rearrangement points. We suggest that at a site of intense transcription, a large 'bubble' of two single DNA strands or an accumulation of more than one, maybe stalled, transcription bubbles occur. DNA breaks on both strands at different positions in the bubble(s) followed by end repair and NHEJ with other chromosomal partner sites. **(A)** to **(G)** chronological order of events. Single DNA strands are represented by light/dark green and red lines, respectively. DNA double strand pairing is represented by short gray lines. After opening of the DNA double strand, two single strand breaks occur that are not complementary to each other, i.e. that are at different sites of the bubble, resulting in a double strand break with about 50 to 550 bases of single strand 5' overhangs. Complementary strands are filled in 5' > 3' by the DNA repair machinery (dashed lines) resulting in a duplication of the single stranded segments. This process can take place at two different loci in the same cell (and same transcriptional hub) and can result in the fusion of different genomic regions by NHEJ **(F)**. **(G)** As a result, both reciprocal fusion products contain the same flanking sequences. ss-break, single strand DNA break. Of note, we observed only in patient YZH that also the non-*TP53* locus (chr. 1) shows duplication of break point-flanking sequences suggesting that the non-*TP53* translocation partner site can have no or short single strand overhangs.

Supplementary Table S1: Sequencing statistics of four OS primary tumors by DNA-PET using the SOLiD platform

Library	Sample	Total beads	Both tags mapped	Span [bp]	Within span	Within span (NR)[1]	Redundancy	Coverage[2]	dPETs[3]	dPET clusters (size 2+)[4]
DHO004HG19	AJF	172,897,363	92,577,911	1510-2570	89,073,088	66,594,042	1.34	46.85	1,383,636	2,278
DHO005HG19	PZP	275,786,428	102,187,549	1910-3060	86,873,155	62,826,184	1.38	53.78	13,893,715	3,811
DHO006DHO008HG19	KRD	286,596,700	168,109,213	660-3980	146,976,367	42,328,532	3.47	23.13	9,695,122	2,733
DHO007DHO009HG19	YZH	378,703,399	167,518,527	1140-4030	147,613,747	60,005,658	2.46	44.98	10,336,682	3,707

[1)]non-redundant paired reads; exclusion of identical PCR amplicons
[2)]physical genome-wide coverage
[3)]discordant mapping paired-end tags
[4)]clusters of dPETs of which their tag one reads and tag 2 reads map to the same regions (regions A and B, respectively), connecting the same two regions

Supplementary Table S2: Statistics of filtering of dPET cluster artifacts before identification of SVs

dPET clusters of size ≥3 before artifact filtering	4737
Filter clusters with superclustersize >40 and UniqueClusterSize <6	218
Blast1 score >2000	265
Blast1 alignment type EC	140
MaxSelfChainLeftCov >80	240
MaxSelfChainRightCov >80	6
Match with simulated library	226
Exclude Overlap	1
dPET clusters of size ≥3 after artifact filtering	3641

For explanation of individual steps see **Materials and Methods** and (Hillmer, Yao et al. 2011; Ng, Hillmer et al. 2012).

Supplementary Table S3: Statistics of germline and somatic SVs identified in four OS tumors

	DHO004HG19	DHO005HG19	DHO006DHO008HG19	DHO007DHO009HG19
	AJF	PZP	KRD	YZH
Deletion	773	603	358	532
Tandem duplication	20	3	11	15
Unpaired inversion	87	72	92	110
Isolated translocation	49	53	129	80
Inversion	33	30	31	39
Insertion	18	30	17	27
Complex rearrangement	68	57	111	193
Total	1,048	848	749	996

Supplementary Table S4: Statistics of somatic SVs identified in four OS tumors

	DHO004HG19	DHO005HG19	DHO006DHO008HG19	DHO007DHO009HG19
	AJF	PZP	KRD	YZH
Deletion	289	177	63	112
Tandem duplication	15	1	7	10
Unpaired inversion	56	46	64	89
Isolated translocation	34	36	119	72
Inversion	3	0	2	4
Insertion	9	6	2	4
Complex rearrangement	28	23	91	129
Total	434	289	348	420

Supplementary Table S5: Statistics of genes affected by somatic SVs of four OS primary tumors

Type of gene alteration	Number of genes
Genes in deletions (<1Mb)	39
Genes in tandem duplications (<1Mb)	2
Genes spanning SVs within one intron	181
Genes spanning SVs affecting coding sequences	31
Fusion genes	67
5' truncated genes	265
3' truncated genes	329

Supplementary Table S6: Somatic SVs of four OS primary tumors (Supplementary Data Set)

Supplementary Table S7: Break point coordinates of *TP53* affecting rearrangements in four OS tumors

Sample	SV ID	Strand left	Validated break left	Strand right	Validated break right	Structural variation	Truncated gene left (strand)	Truncated gene right (strand)	Predicted fusion gene or mode of truncation
AJF	D38	+	chr17:7,557,506	+	chr17:7,651,285	deletion	*ATP1B2*(+)	*DNAH2*(+)	*ATP1B2-DNAH2*
KRD	CT54	+	chr5:137,520,904	+	chr17:7,586,797	complex inter-chr.	*KIF20A*(+)	*TP53*(–)	2 x 3' truncation
KRD	CT7	–	chr6:36,559,119	+	chr17:7,588,049	complex inter-chr.	–	*TP53*(–)	3' truncation
KRD	CT15	+	chr1:172,555,688	–	chr17:7,588,094	complex inter-chr.	*SUCO*(+)	*TP53*(–)	*SUCO-TP53*
PZP	T5	–	chr6:132,198,801[1)]	+	chr17:7,586,884[1)]	insertion inter-chr.	*ENPP1*(+)	*TP53*(–)	*TP53-ENPP1*[2)]
PZP	T12	+	chr6:132,211,834	–	chr17:7,586,948	insertion inter-chr.	*ENPP1*(+)	*TP53*(–)	*ENPP1-TP53*[2)]
YZH	T6	–	chr1:226,260,906	+	chr17:7,587,974	isolated translocation	–	*TP53*(–)	3' truncation
YZH	T13	+	chr1:226,261,198	–	chr17:7,588,529	isolated translocation	–	*TP53*(–)	5' truncation

[1)]DNA-PET mapping coordinates; rearrangement point could not be amplified by PCR
[2)]One fusion transcript based on an insertion of a part of *ENPP1* into *TP53* (see Figure S5)

Supplementary Table S8: Bone-forming tumors or tumor-like lesions other than OS

Diagnosis	*n*	Diagnosis	*n*
Fibrous dysplasia	42/50	Fibrocartilaginous mesenchymoma	4/4
Aneurysmal bone cyst	14/17	Nora lesion	2/2
Osteoid osteoma	14/15	Osteofibrous dysplasia	2/2
Ossifying fibroma	13/15	Osseous dysplasia	2/2
Reactive bone formation	12/13	Desmoplastic fibroma	2/2
Osteoblastoma	8/8	Adamantinoma	1/1
Myositis ossificans	7/9	Non-ossifying fibroma	1/1

n = number of evaluable cases/total number of cases

Supplementary Table S9: Overall survival of TMA OS patients stratified for *TP53* FISH signal and protein expression

Overall survival	5 years	10 years
TP53 FISH		
FISH negative (*n* = 192)	61.20%	58.70%
FISH positive (*n* = 23)	64.90%	64.90%
TP53 immunhistochemistry		
IHC negative (*n* = 170)	59.80%	57.10%
IHC positive (*n* = 42)	59.20%	54.30%

Supplementary Table S10: TMA content and result of *TP53* FISH analysis

Tissue type	*n*
Adrenal gland, adenoma	4/4
Brain, astrocytoma	11/12
Brain, glioblastoma	15/17
Brain, Meningeoma	14/15
Brain, normal	1/1
Brain, oligodendroglioma	5/5
Breast, ductal carcinoma	18/20
Breast, lobular carcinoma	16/18
Breast, medullary carcinoma	21/24
Breast, mucinous carcinoma	7/8
Breast, normal	1/1
Breast, tubular carcinoma	8/9
Cervix, *in situ* carcinoma	10/11
Colon, adenoma	41/46
Colon, carcinoma	21/24
Colon, normal	0/0
Endometrium, endometrioid carcinoma	12/13
Endometrium, normal	1/1
Endometrium, serous carcinoma	11/11
Esophagus, adenocarcinoma	3/3
Esophagus, normal	2/2
Esophagus, small cell carcinoma	1/1
Esophagus, squamous cell carcinoma	7/8
Fat tissue, normal	0/0
Gall bladder, carcinoma	12/13
Gall bladder, normal	5/6
Heart, normal	4/4

(*Continued*)

Tissue type	*n*
Kidney, chromophobe carcinoma	2/3
Kidney, clear cell carcinoma	24/27
Kidney, normal	3/3
Kidney, oncocytoma	8/8
Kidney, papillary carcinoma	11/12
Larynx, carcinoma	13/14
Liver, hepatocellular carcinoma	28(32
Liver, normal	5/5
Lung, adenocarcinoma	54/61
Lung, large cell carcinoma	15/17
Lung, normal	4/5
Lung, small cell carcinoma	15/15
Lung, squamous cell carcinoma	30/32
Lymph node, Hodgkin Lymphoma	15/18
Lymph node, non Hodgkin Lymphoma	18/19
Lymph node, normal	2/2
Mesothelioma	13/14
Myometrium, normal	2/2
Myometrium, myoma	18/22
Nerve, neurofibroma	12/14
Nerve, schwannoma	8/9
Oral cavity, carcinoma	18/21
Oral cavity, normal	5/5
Ovary, endometrioid carcinoma	18/20
Ovary, mucinous carcinoma	3/3
Ovary, normal	0/0
Ovary, serous carcinoma	17/18
Pancreas, adenocarcinoma	14/15
Pancreas, normal tissue	4/6
Paraganglioma	5/6
Parathyroid, adenoma	17/21
Parathyroid, normal	0/0
Pheochromozytoma	10/11
Prostate, adenocarcinoma	33/37
Prostate, normal	9/9
Salivary gland, cylindroma	11/11
Salivary gland, normal	6/6

(*Continued*)

Tissue type	*n*
Salivary gland, pleomorphic adenoma	16/18
Salivary gland, Warthin tumor	7/8
Skeletal muscle, normal	2/3
Skin, basal cell carcinoma	23/27
Skin, histiocytoma	9/10
Skin, Kaposi sarcoma	8/9
Skin, melanoma	32/36
Skin, naevus	22/24
Skin, normal	4/4
Skin, squamous cell carcinoma	10/10
Small intestine carcinoma	8/9
Small intestine, normal	0/0
Soft tissue, giant cell tumor of tendon sheath	10/11
Soft tissue, hemangioma, capillary type	6/6
Soft tissue, leiomyosarcoma	13/15
Soft tissue, lipoma	5/5
Soft tissue, liposarcoma	6/6
Soft tissue, pleomorphic sarcoma	9/10
Stomach, carcinoma, diffuse type	7/8
Stomach, carcinoma, intestinal type	14/17
Stomach, normal	4/5
Testis, non-seminomatous carcinoma	16/20
Testis, normal	3/3
Testis, seminoma	14/14
Thymus, normal	1/1
Thymus, thymoma	8/8
Thyroid, adenoma	11/12
Thyroid, follicular carcinoma	12/13
Thyroid, normal	1/1
Thyroid, papillary carcinoma	5/5
Urinary bladder, invasive carcinoma	10/11
Urinary bladder, non-invasive carcinoma	10/10
Urinary bladder, normal	15/16
Vulva, squamous cell carcinoma	8/8
Total tumor	**966/1072**
Total normal	**84/91**
Total tumor + normal	**1,050/1,163**

n = number of evaluable cases/total number of cases

Supplementary Table S11: Summary of TMA *TP53* FISH analysis

Kind of tissue	*n*
Normal tissue	84/91
Brain tumors	45/49
Breast tumors	70/79
Gynecologic tumors	97/106
Genitourinary tumors	128/142
Others	118/131
Gastrointestinal tumors	208/234
Lung tumors	114/125
Lymphoid tumors	33/37
Skin tumors	104/116
Soft tissue tumors	49/53
Total	**1,050/1,163**

n = number of evaluable cases/total number of cases

Supplementary Table S12: Copy number variations of two affected LFS family members based on CytoScan array analysis

Patient	CN[1] State	Type	Chr	Min[2]	Max[2]	Size (kb)	Marker Count	Confidence	Genes	Comment for CNV shared between patient 1 and 2
1	0	Loss	2	41,239,606	41,250,106	10.5	5	0.9954		
1	1	Loss	2	168,172,736	168,180,626	7.89	11	0.9297		
13	1	Loss	2	168,172,736	168,180,626	7.89	11	0.9623		
1	1	Loss	3	160,772,598	160,778,822	6.224	9	0.9388	PPM1L	
13	3	Gain	4	132,780,784	132,894,269	113.485	45	0.8855		
1	3	Gain	5	32,108,414	32,162,756	54.342	53	0.9247	PDZD2, GOLPH3	CNV site in DGV
13	3	Gain	5	32,108,414	32,166,970	58.556	55	0.9186	PDZD2, GOLPH3	CNV site in DGV
13	1	Loss	7	3,833,336	3,852,657	19.321	14	0.9512	SDK1	
13	0	Loss	8	39,234,303	39,357,501	123.198	8	1.0000	ADAM5P, ADAM3A	
13	1	Loss	8	84,367,320	84,380,551	13.231	11	0.9519		
1	1	Loss	8	96,076,737	96,098,249	21.512	14	0.9106	MIR3150	CNV site in DGV
13	1	Loss	8	96,076,737	96,098,249	21.512	14	0.9538	MIR3150	CNV site in DGV
13	3	Gain	12	32,005,944	32,062,001	56.057	40	0.9289		
1	1	Loss	12	69,023,587	69,032,212	8.625	9	0.9250	RAP1B	
13	3	Gain	14	106,022,513	107,051,759	1029.25	23	0.9158	KIAA0125, ADAM6, NCRNA00226, NCRNA00221	

(*Continued*)

Patient	CN[1] State	Type	Chr	Min[2]	Max[2]	Size (kb)	Marker Count	Confidence	Genes	Comment for CNV shared between patient 1 and 2
13	1	Loss	15	20,175,623	22,504,198	2328.58	48	0.8801	HERC2P3, GOLGA6L6, GOLGA8C, BCL8, POTEB, NF1P1, LOC646214, CXADRP2, LOC727924, OR4M2, OR4N4, OR4N3P	CNV site in DGV
1	1	Loss	15	22,300,190	22,504,198	204.008	38	0.8682	LOC727924, OR4M2, OR4N4, OR4N3P	CNV site in DGV
13	3	Gain	16	34,455,753	34,762,298	306.545	84	0.9135	LOC283914, LOC146481, LOC100130700	
13	1	Loss	17	28,303,998	28,317,131	13.133	18	0.9198	EFCAB5	
1	1	Loss	18	1,722,426	1,838,901	116.475	110	0.9158		
13	3	Gain	18	51,345,688	51,423,648	77.96	57	0.9415		
13	3	Gain	19	20,833,215	20,987,762	154.547	123	0.9063	ZNF626	
13	1	Loss	19	28,294,543	28,318,358	23.815	15	0.9048		
13	3	Gain	19	58,364,597	58,383,708	19.111	20	0.9187	ZNF587, ZNF814	
1	1	Loss	20	32,806,979	32,822,219	15.24	9	0.9050		
13	3	Gain	22	22,861,993	23,358,013	496.02	65	0.9360	ZNF280B, ZNF280A, PRAME, LOC648691, POM121L1P, GGTLC2, MIR650, IGLL5	
1	2	Gain	X	2,706,943	2,713,139	6.196	2	0.2191	XG	
1	2	Gain	X	58,094,436	62,058,620	3964.18	19	0.2466		
1	4	Gain	X	150,192,436	150,195,253	2.817	8	0.9315		

[1]Copy number
[2]Position based on NCBI human reference Build 37

REFERENCES

1. Krzywinski M, Schein J, Birol I, Connors J, Gascoyne R, Horsman D, Jones SJ, Marra MA. Circos: an information aesthetic for comparative genomics. Genome Research. 2009; 19:1639–1645.
2. Rhead B, Karolchik D, Kuhn RM, Hinrichs AS, Zweig AS, Fujita P a, Diekhans M, Smith KE, Rosenbloom KR, Raney BJ, Pohl A, Pheasant M, Meyer LR, et al. The UCSC Genome Browser database: update 2010. Nucleic Acids Research. 2010; 38:D613–619.
3. Djebali S, Davis C, Merkel A, Dobin A. Landscape of transcription in human cells. Nature. 2012; 489:101–108.